IEEE Photonics Journal
An IEEE Photonics Society Publication

Experimental Demonstrations and Extensive Comparisons of End-to-End Real-Time Optical OFDM Transceivers With Adaptive Bit and/or Power Loading

Volume 3, Number 3, June 2011

X. Q. Jin
J. L. Wei
R. P. Giddings
T. Quinlan
S. Walker
J. M. Tang

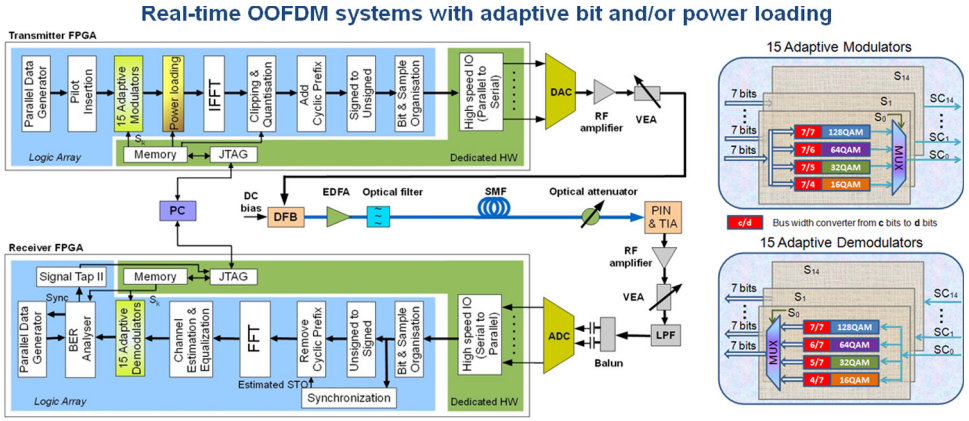

DOI: 10.1109/JPHOT.2011.2154380
1943-0655/$26.00 ©2011 IEEE

IEEE photonics SOCIETY

IEEE

Experimental Demonstrations and Extensive Comparisons of End-to-End Real-Time Optical OFDM Transceivers With Adaptive Bit and/or Power Loading

X. Q. Jin,[1] J. L. Wei,[1] R. P. Giddings,[1] T. Quinlan,[2] S. Walker,[2] and J. M. Tang[1]

[1]School of Electrical Engineering, Bangor University, LL57 1UT Bangor, U.K.
[2]School of Computer Science and Electronic Engineering, University of Essex, CO4 3SQ Colchester, U.K.

DOI: 10.1109/JPHOT.2011.2154380
1943-0655/$26.00 ©2011 IEEE

Manuscript received April 4, 2011; revised May 6, 2011; accepted May 7, 2011. Date of publication May 12, 2011; date of current version May 27, 2011. This work supported in part by the European Community's Seventh Framework Program under FP7/2007-2013 within the project ICT ALPHA under Grant agreement 212 352 and in part by the Welsh Assembly Government and The European Regional Development Fund. Corresponding author: X. Q. Jin (e-mail: x.jin@bangor.ac.uk).

Abstract: Experimental demonstrations are reported for end-to-end real-time optical orthogonal frequency division multiplexing (OOFDM) transceivers incorporating three widely adopted adaptive loading techniques, namely, power loading (PL), bit loading (BL), and bit-and-power loading (BPL). In directly modulated distributed-feedback (DFB) laser-based, intensity-modulation, and direct-detection (IMDD) transmission systems consisting of up to 35-km single-mode fibers (SMFs), extensive experimental comparisons between these adaptive loading techniques are made in terms of maximum achievable signal bit rate, optical power budget, and digital signal processing (DSP) resource usage. It is shown that BPL is capable of supporting end-to-end real-time OOFDM transmission of 11.75 Gb/s over 25-km SMFs in the aforementioned systems at sampling speeds as low as 4 GS/s. In addition, experimental measurements also show that BPL (PL) offers the highest (lowest) signal bit rate, and their optical power budgets are similar. The observed signal bit rate difference between BPL and PL is almost independent of sampling speed and transmission distance. All the aforementioned key features agree very well with numerical simulations. On the other hand, BPL-consumed DSP resources are approximately three times higher than those required by PL. The results indicate that PL is a preferred choice for cost-effective OOFDM transceiver design.

Index Terms: Adaptive loading, fiber optics systems, optical modulation, orthogonal frequency division multiplexing (OFDM).

1. Introduction

Optical orthogonal frequency division multiplexing (OOFDM) is considered to be a promising technique for practical implementation in next-generation optical networks of various architectures [1]–[11], as it has a number of inherent and unique advantages including high spectral efficiency, great resistance to linear system impairments, and provision of hybrid dynamic bandwidth allocation in both the frequency and time domains. For cost-sensitive OOFDM passive optical network (PON) application scenarios of interest in the present paper, low-cost electrical and optical components are always preferred, whose bandwidths are, however, usually very narrow. For example, in the electrical domain, digital-to-analog converters (DACs) employed in real-time OOFDM transceivers

[1], [2] exhibit analog frequency response roll-offs as large as 6 dB within the 2-GHz signal spectral region. Inevitably, this causes significant variations in achievable signal-to-noise ratios (SNRs) experienced by the subcarriers. On the other hand, in the optical domain, the use of small modulation bandwidth intensity modulators such as vertical-cavity surface-emitting laser (VCSEL) intensity modulators [1] and reflective semiconductor optical amplifier (RSOA) intensity modulators [2] can further increase the system frequency response roll-off effect.

To effectively combat the aforementioned system frequency response roll-off effect and subsequently improve the transmission performance of the OOFDM PON system, adaptive loading can be adopted, which fully uses OOFDM subcarrier orthogonality to independently manipulate bits and/or electrical power of each individual subcarrier through negotiations between the transmitter and receiver [3]–[10]. In general, more bits and/or less electrical power are applied to a subcarrier with a high SNR or less distortion, and zero powers are assigned to subcarriers in deep fade. The optimum bits and/or electrical power assigned on each subcarrier are determined mainly by the properties of the transmission system frequency response.

There are three classes of adaptive loading techniques: bit loading (BL) [3]–[5], power loading (PL) [6], [7], and bit-and-power loading (BPL) [8]–[10]. In the BL technique, different signal modulation formats are taken on individual subcarriers having identical electrical powers. In the PL technique, electrical subcarrier powers are manipulated with the same signal modulation formats being taken on all the subcarriers. Finally, in the BPL technique, both the electrical power and signal modulation format taken on each individual subcarrier are adjusted independently. Each of these adaptive loading techniques can be employed to maximize the signal bit rate for a given bit error rate (BER) and a fixed power constraint or to minimize the BER for a given signal bit rate to improve the system power budget. Throughout the present paper, the option of maximizing the signal bit rate at a forward error correction (FEC) threshold BER of 1.0×10^{-3} is considered.

Over the past several years, the aforementioned three adaptive loading techniques have been extensively investigated, both theoretically and experimentally, for various OOFDM system configurations [3]–[11]. Experimental measurements using offline digital signal processing (DSP) have shown [4] that the BL technique can support 12.5-Gb/s OOFDM signal transmission over 20-km single-mode fibers (SMFs) in intensity-modulation and direct-detection (IMDD) systems, while the BPL technique can offer a maximum 47.4-Gb/s OOFDM signal transmission over 100-m graded-index plastic optical fibers (GI-POFs) [8]. More importantly, in end-to-end real-time OOFDM transmission systems, by employing the PL technique, an 11.25-Gb/s OOFDM signal transmission has been experimentally demonstrated successfully over 25-km standard and MetroCor SMF-based IMDD systems using directly modulated distributed-feedback (DFB) lasers (DMLs) [6]. These investigations indicate that, to maximize the transmission performance, adaptive loading is effective not only in fully utilizing the available system frequency response characteristics determined by system/network elements but in combating nonlinear component impairments as well.

It should be pointed out, as discussed in Section 6 of the present paper, that the BPL technique has the ability of achieving the largest signal bit rate, but it suffers from the highest level of computational complexity and requires sophisticated OOFDM transceiver designs to accommodate the variations in both the number of bits per symbol and the selective modulation formats. On the other hand, the PL technique has the least computational complexity and requires the simplest OOFDM transceiver architectures. As a direct result, the PL technique has been experimentally implemented successfully in end-to-end real-time OOFDM transceivers at 11.25-Gb/s, using low-cost, off-the-shelf, electrical and optical components [6].

For a specific application scenario, to provide an effective means of selecting an optimum adaptive loading technique in OOFDM transceiver design to effectively offset the transceiver complexity by its transmission performance, detailed performance explorations of these three adaptive loading techniques have been undertaken theoretically over 1000 statistically constructed worst case multimode fiber (MMF) systems [11]. It has been shown that, for the majority of practical cases, relative signal bit rate differences between the most sophisticated BPL technique and the simplest PL technique are approximately 7% [11].

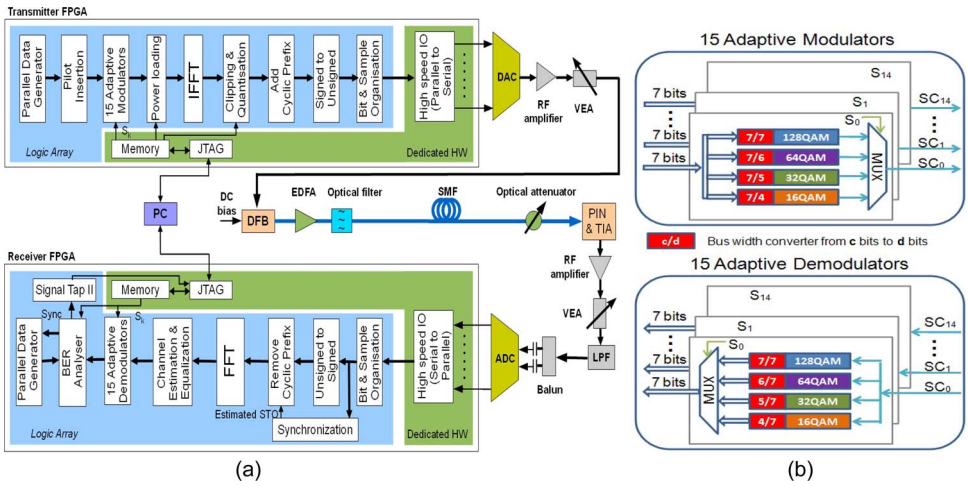

Fig. 1. (a) End-to-end real-time OOFDM system with adaptive bit and/or power loading capability. VEA: Variable electrical attenuator. LPF: Low-pass filter. STO: Symbol timing offset. (b) Block diagrams for 15 parallel adaptive QAM modulators/demodulators. SC: Subcarrier.

To experimentally verify the theoretical prediction reported in [11], in this paper, use is made of end-to-end real-time OOFDM transceivers with adaptive bit and/or power loading capability reported in [12] to extensively compare these three adaptive loading techniques in terms of i) BER versus received optical power performance; ii) DAC/ADC sampling speed-dependent signal bit rate; iii) transmission distance-dependent signal bit rate, and iv) DSP resource usage. In all these experimental investigations, simple DML-based IMDD SMF systems are considered, and adaptive loading is realized using live transceiver parameter optimization according to online measured subcarrier and total channel BERs. It is shown that the BPL technique is capable of supporting 11.75-Gb/s OOFDM signal transmission over 25-km MetroCor SMF-based IMDD systems using DMLs. More importantly, BPL (PL) offers the highest (lowest) signal bit rate, and their optical power budgets are similar. The absolute signal bit rate difference between BPL and PL is almost independent of both DAC/ADC sampling speed and transmission distance under the experimental conditions adopted in the paper. All the aforementioned key features agree very well with not only the theoretical predictions based on worst-case MMFs for cases where cyclic prefixes are sufficiently long for compensating the system linear impairments [11] but with the numerical simulations performed here in DML-based IMDD SMF systems as well. In addition, based on the compilation report, detailed comparisons of resource usage are also made between different adaptive loading techniques. Results show that BPL-consumed DSP resources are approximately three times higher than those required by PL. The present paper strongly indicates that the PL technique is sufficiently effective in escalating the OOFDM system performance to its maximum potential for the majority of transmission systems encountered in practice. The statement may have great potential for cost-effective OOFDM transceiver designs. Here, it is worth mentioning that the adaptive loading technique demonstrated in the present paper is also applicable in coherent transmission systems, which may, however, not be cost-effective for PON applications.

2. Real-Time OOFDM Systems With Adaptive Bit and/or Power Loading

Fig. 1(a) shows the diagram of the considered end-to-end real-time OOFDM transmission system with adaptive bit and/or power loading capability. As detailed descriptions have already been made of its key functionalities including the inverse Fast Fourier transform (IFFT)/FFT, channel estimation/equalization, symbol synchronization, online performance monitoring, and live parameter optimization [6], [7], here, special attention is, therefore, given to the implementation of adaptive bit and/or power loading techniques in real-time OOFDM transceivers. In this paper, use is made of 15 subcarriers to convey user data, and the signal modulation format taken on each individual

subcarrier may vary from 16-quadrature amplitude modulation (QAM), 32-QAM, 64-QAM, and 128-QAM. Both online subcarrier/system performance monitoring and live optimizations of subcarrier bit allocation and/or subcarrier powers, as well as live optimizations of component/system operating conditions, are performed using the FPGA embedded logic analyzer and memory editor via a joint test action group (JTAG) connection to a personal computer. The main internal clock is 100 MHz, which is identical to the OOFDM symbol rate.

In the transmitter, to realize adaptive BL and simultaneously maintain the input data interface at a fixed bit width, regardless of the selected signal modulation formats, for each subcarrier, an adaptive modulator consisting of four parallel 16-QAM, 32-QAM, 64-QAM, and 128-QAM modulators is employed, as shown in Fig. 1(b). At the input of each of these parallel modulators, a bus bit converter is also implemented, which pads a certain number of extra "0" bits into the original user bits allocated to the subcarrier to construct a data interface at a constant bit width and, before signal encoding, extracts only the user bits by removing the padded extra "0" bits. In the present transceiver design, the bit width for each subcarrier is fixed at 7, which corresponds to the highest possible signal modulation format of 128-QAM. For a specific subcarrier, the exact number of extra "0" bits padded by the corresponding bus bit converter is determined by the modulator selected by the feedback information S_k. The feedback information is generated via negotiations between the transmitter and the receiver and represents the transmission channel characteristics. Based on the above descriptions, it is easy to understand that, for the present transceiver, the total bit width of the input data interface is $105 (= 15 \times 7)$ bits, which include user data bits, padded "0" bits, and fixed pilot bits. On the other hand, in the receiver, a similar adaptive demodulator for each subcarrier is implemented, which performs an inverse of the aforementioned transmitter DSP according to the same feedback information S_k. All the padded extra "0" bits are then discarded after the output data interface in the receiver.

Here, the following two important aspects are worth mentioning: a) Not all of the padded extra "0" bits participate in the signal transmission over the fiber systems, as these bits are completely removed prior to signal encoding in the transmitter and restored back after signal decoding in the receiver to retain a fixed interface input/output bit width. b) As mentioned previously, the feedback information S_k, originating from the online-controlled internal memory, is generated via negotiations between the transmitter and the receiver to control the selection of an optimum modulator/demodulator for a subcarrier and, subsequently the number of padded "0" bits. This provides the OOFDM transceivers with the desired unique capability of adapting transmission system characteristics.

In the transmitter, for each subcarrier PL is realized by individually multiplying the encoded digital complex number by an online controlled gain coefficient to adaptively vary the subcarrier amplitude, as shown in Fig. 1(a). After applying the PL technique to all the 15 parallel subcarriers, to generate real-valued OFDM symbols, the IFFT is performed to these 15 subcarriers and one zero-frequency subcarrier having a zero power, together with their 16 complex conjugate counterparts being arranged to satisfy the Hermitian symmetry. The output amplitude of the IFFT is first scaled to a fixed level with an optimum clipping ratio and then quantized to 8-bits to match the resolution of the employed DAC.

A cyclic prefix of eight samples is added to each OFDM symbol, giving rise to 40 samples per symbol. The signed samples are then converted to unsigned ones by adding an appropriate DC offset. After performing sample ordering and bit arrangement, the unsigned 40 samples are streamed to the DAC interface. The DAC generates an analog electrical OFDM signal having a maximum peak-to-peak voltage of 636 mV; then, the OFDM signal is then amplified or attenuated as necessary and subsequently combined with an optimum DC bias current; it is finally injected into an 1550-nm DML with a 3-dB modulation bandwidth of approximately 10 GHz and a threshold current of 29 mA. The optimum driving voltage is approximately 0.4 Vpp, and the optimum bias current is 36 mA, and corresponding to this the DML optical output power is approximately -3.5 dBm.

The OOFDM signal emerging from the DML is coupled into an erbium-doped fiber amplifier (EDFA) with a 15-dB optical gain and a 5-dB noise figure. After passing through a 0.8-nm optical

filter, the amplified optical signal is coupled into the MetroCor SMFs at a fixed optical launch power of 7 dBm. It should be noted that the use of the EDFA is to vary the optical launch power only.

In the receiver, after passing through an optical attenuator, the received OOFDM signal is converted into the electrical domain using an MMF-pigtailed 12-GHz PIN with TIA. The PIN has a receiver sensitivity of -17 dBm (corresponding to 10-Gb/s nonreturn-to-zero data at a BER of 1.0×10^{-9}). The converted electrical signal is first amplified with a 2.5-GHz, 20-dB RF amplifier and then attenuated as needed to optimize the signal amplitude to suit the input range of the ADC. After the 8-bit ADC and a serial-to-parallel converter, the parallel samples undergo a number of DSP procedures, including symbol synchronization, FFT, channel estimation and equalization, as well as adaptive demodulation.

As the feedback information that is identical to that used in the transmitter is employed in the receiver, the user bits loaded in the transmitter are extracted after the adaptive demodulators for error counting in the BER analyzer. The bit error count over 88 500 symbols is continuously updated and displayed with the embedded logic analyzer for the entire transmission channel, as well as for each individual subcarrier over a defined measurement time period. This enables fine and live adjustment of transceiver/system parameters to maximize the system performance.

3. OOFDM System Modeling and Simulation Parameters

To gain an in-depth insight into the experimental results, detailed numerical simulations of the transmission performance of the considered real-time OOFDM DML-based IMDD systems incorporating different adaptive loading techniques are also undertaken based on a comprehensive theoretical OOFDM system model presented in [13]. The theoretical OOFDM system model contains the following major elements: an electrical OFDM transmitter for electrical OFDM signal generation, a DML for intensity modulation, an SMF for optical signal transmission, a variable optical attenuator, a square-law photon detector, an electrical low-pass filter (LPF), and an electrical OFDM receiver for signal recovery. In addition, adaptive bit and/or power loading is simulated following the procedure detailed in [11]. The validity of the OOFDM system model has been rigorously verified at both component and system levels [3], [6], [13]–[15]. As electrical OFDM signal generation and data recovery used in numerical simulations follow the procedures described in Section 2, and similar procedures have also been presented in [3] and [13], in this section, brief discussions are, therefore, made of the theoretical models of DMLs, SMFs, PINs, and LPFs only.

To simulate the nonlinear properties of the DFB-based DML, a lumped theoretical DFB laser model developed in [14] is adopted, taking into account a wide diversity of nonlinear effects, namely, longitudinal-mode spatial hole-burning, linear and nonlinear carrier recombination, as well as nonlinear optical gain. It is also assumed that the influence of the laser linewidth on the system performance is negligible. Such an assumption holds well for the transmission systems considered here [16]. For simulating the DFB laser operating at 1550 nm, the parameters identical to those reported in [13] are adopted: a cavity length of 300 μm; a cross-sectional area of the active region of 0.066 μm^2; a photon lifetime of 3.6 ps; a nonlinear gain coefficient of 7.4×10^{-23} m^3; a linewidth enhancement factor of 3; a transparency carrier density of 1.5×10^{24} m^{-3}; a carrier lifetime of 10 ns; a bimolecular recombination coefficient of 1.0×10^{-16} m^3/s; an Auger recombination coefficient of 6.5×10^{-41} m^6/s; a linear gain coefficient of 7.5×10^{-20} m^2; an optical width (vertical) of 0.47 μm; an optical width (horizontal) of 1.80 μm; a confinement factor of 0.07; a group refractive index of 3.7; a phase refractive index of 3.2203; and a 38% coupling efficiency from the laser chip to the SMF.

A standard theoretical SMF model successfully used in [3], [6], [13], and [15] is employed, in which the effects of loss, chromatic dispersion, and optical power dependence of refractive index are taken into account. The effect of fiber nonlinearity-induced phase noise to intensity noise conversion is also included. The SMF parameters are listed as follows: an effective area of 80 μm^2, a dispersion parameter of 18.0 ps/nm/km, a dispersion slope of 0.07 ps/nm^2/km, a loss of 0.20 dB/km, and a Kerr coefficient of 2.35×10^{-20} m^2/W.

A square-law photon detector is employed in the receiver to detect the optical signals emerging from the transmission systems. Both shot noise and thermal noise are considered, which are

simulated following the procedures similar to those presented in [17], taking into account parameter values similar to those corresponding to the PIN adopted in the present experimental measurements.

An electrical LPF is considered, which has the amplitude and phase responses similar to those employed in the experimental measurements. The LPF introduces both the system frequency response roll-off and frequency-dependent phase variation to the received electrical OFDM signals.

It should be noted, in particular, that all the component and system parameters mentioned in Section 2 are used in the numerical simulations, and other parameters that are not made known in the experiments are taken from [13].

4. Boundary Conditions for Implementing Adaptive Loading Techniques

As already mentioned in Section 1, the key focus of the present paper is to compare the capability of different adaptive loading techniques in achieving a maximum signal bit rate $C_{\max}$ at a total channel BER of 1.0×10^{-3}

$$C_{\max} = Max\left(\sum_{k=1}^{15} b_k \Big/ T_s\right) \tag{1}$$

where b_k is the number of bits loaded on kth subcarrier within one OFDM symbol, and T_s is the symbol time period with the cyclic prefix region being excluded. In both numerical simulations and experimental measurements, for fair comparisons between three adaptive loading techniques, the following two boundary conditions must be satisfied simultaneously:

- The total electrical signal powers remain at identical values for all the adaptive loading techniques. For the transmission system considered here, this results in a fixed optimum signal clipping ratio of approximately 12 dB [18].
- The resulting maximum signal bit rates are valid only when the corresponding total channel BERs are $< 1.0 \times 10^{-3}$.

In implementing BL (PL), the procedure reported in [3] (see [6]) is adopted, in which the modulation format (power) taken on each subcarrier is varied iteratively according to the corresponding subcarrier BER. While implementing BPL, PL is first applied to satisfy the above two boundary conditions, based on a highest possible signal modulation format across all subcarriers. After that, according to the resulting subcarrier BER distribution and the loaded/received subcarrier power profile, the modulation format and power taken on the subcarrier is adjusted again to further maximize the signal bit rate with the two boundary conditions being still met.

It should be noted that subcarriers are dropped completely when one of the following cases is encountered.

- For the BL (PL) technique, subcarriers with the lowest modulation formats (the highest powers) still suffer excessive errors to achieve the required total channel BER of 1.0×10^{-3}.
- For the BPL technique, subcarriers with the lowest modulation formats and the highest powers still suffer excessive errors to achieve the required total channel BER of 1.0×10^{-3}.

5. Results

5.1. Examples of Measured Optimum Subcarrier Bit and Power Profiles

For these three adaptive loading techniques, examples of measured optimum profiles of loaded/received subcarrier powers, optimum bits allocated on each subcarrier, and the resulting subcarrier BER distributions are shown in Fig. 2 for DML-based IMDD 25-km SMF transmission systems using DACs/ADCs at sampling speeds of 4 GS/s. In Fig. 2(a), the loaded/received subcarrier powers are normalized to the corresponding maximum loaded/received subcarrier powers. At the sampling speeds of 4 GS/s, the maximum signal bit rates achieved using BL, PL, and BPL are 10.375 Gb/s, 11.25 Gb/s, and 11.75 Gb/s, respectively. However, as shown in Fig. 4, PL gives the lowest signal bit rates for sampling speeds of < 4 GS/s. Here, the choice of 4 GS/s demonstrates the maximum achievable signal bit rates for different adaptive loading techniques.

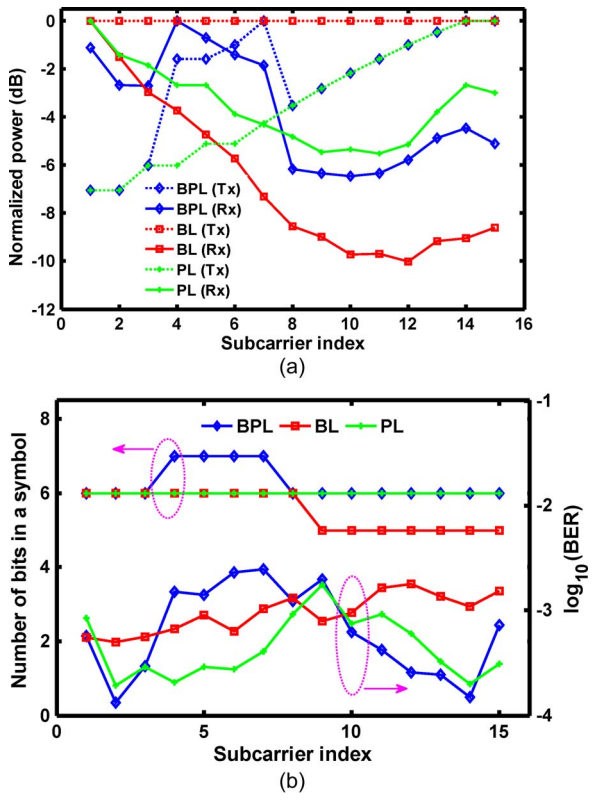

Fig. 2. (a) Examples of experimentally measured optimum profiles of loaded/received subcarrier powers normalized to the corresponding maximum loaded/received subcarrier power. (b) Optimum bits allocated on each subcarrier and resulting subcarrier BER distributions. In both cases, DML-based IMDD 25-km SMF systems using DACs/ADCs at sampling speeds of 4 GS/s are considered.

It can be seen in Fig. 2(a) that, of these three adaptive loading techniques, the BL-enabled constant loaded subcarrier power profile in the transmitter gives rise to the largest received subcarrier power variation of approximately 10 dB within the 2-GHz signal spectrum region. The received subcarrier power variation occurs due to the system frequency response roll-off effect, resulting from the following three mechanisms [1], [6]: i) DAC analog frequency response roll-off; ii) DML intensity modulation nonlinearity, and iii) IMDD nature of the transmission system. As a direct result of the system frequency response roll-off effect, 64-QAM (6 bits) is used on the first eight low-frequency subcarriers, suffering relatively low transmission losses, while 32-QAM (5 bits) is used on the remaining seven high-frequency subcarriers experiencing relatively high transmission losses, as observed in Fig. 2(b). The aforementioned optimum subcarrier bit allocation results in an almost uniformly distributed BERs across all the subcarriers, as demonstrated in Fig. 2(b), also producing a total channel BER of $< 1.0 \times 10^{-3}$.

On the other hand, when PL is adopted, to obtain a uniform subcarrier BER distribution and a total channel BER of $< 1.0 \times 10^{-3}$, the highest possible signal modulation format of 64-QAM is taken on each subcarrier, as shown in Fig. 2(b). To compensate the system frequency response roll-off effect discussed above, the loaded subcarrier power increases with increasing subcarrier frequency, as seen in Fig. 2(a). The maximum achievable variation range of the loaded subcarrier power is determined by the dynamic power range of the IFFT and quantization noise. In addition, Fig. 2(a) also shows that the loaded subcarrier powers in the low-frequency region (first and second subcarriers) are very similar. The physical mechanism underpinning the loaded subcarrier power similarity between the first two subcarriers is subcarrier $\times$ subcarrier intermixing upon direct detection in the receiver [6], [18]. As the intermixing effect increases almost linearly with decreasing

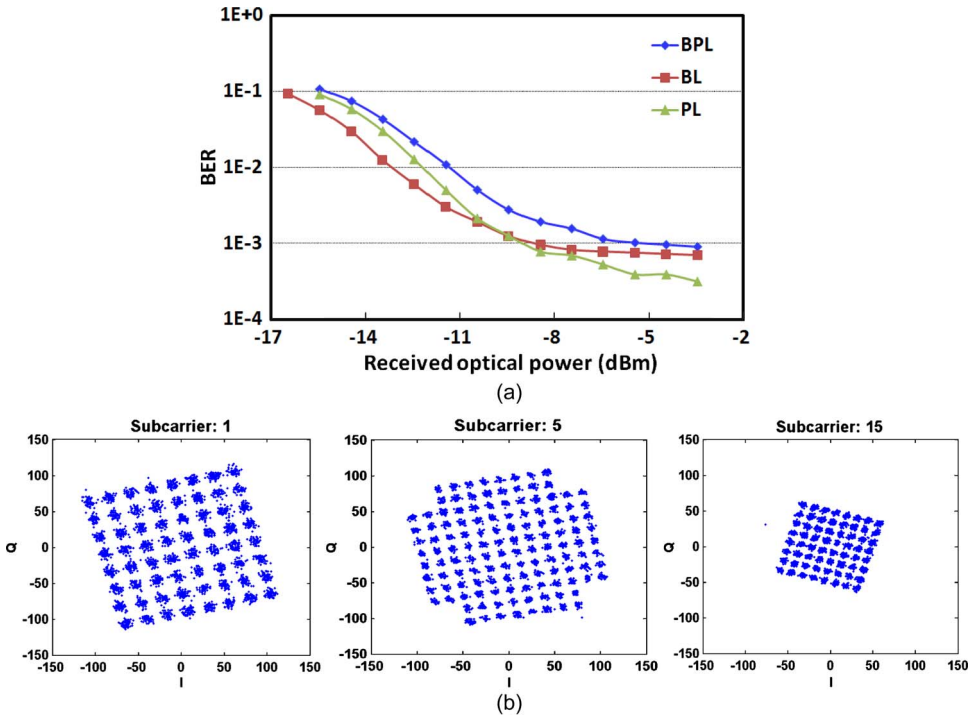

Fig. 3. Transmission performance of end-to-end real-time OOFDM transceivers with various adaptive loading techniques over DML-based IMDD 25-km SMF systems using DACs/ADCs at sampling speeds of 4 GS/s. (a) BER performance. (b) Received constellations of single subcarriers before equalization in the receiver.

subcarrier frequency, relatively high loaded subcarrier powers are thus required for the low-frequency subcarriers to effectively combat the intermixing effect.

Finally, making use of the PL-enabled loaded/received subcarrier power profile and considering the corresponding subcarrier BER distribution, BPL is introduced to manipulate both the loaded subcarrier power and bit allocation for each subcarrier. As shown in Fig. 2(b), the signal modulation formats taken on subcarriers with indices from 4 to 7 are increased to 128-QAM (7 bits), while 64-QAM is still retained for all other subcarriers. Apart from the aforementioned optimum bit allocation, the subcarrier powers loaded on the subcarriers encoded using 128-QAM grows by about 2 dB, compared with the PL case. The occurrence of the increased signal modulation format level for these subcarriers is due to the coexistence of the effects of subcarrier $\times$ subcarrier intermixing and system frequency response roll-off; with increasing subcarrier frequency, the first effect becomes weak, while the second effect becomes strong. Thus, an optimum spectral region occurs, over which subcarriers suffer the least distortions to enable the use of 128-QAM.

5.2. BER Versus Received Optical Power Performance

Based on the optimum loaded subcarrier power profile and/or subcarrier bit allocation identified in Section 5.1 for each adaptive loading technique, experimental measurements are undertaken of the transmission performance of the end-to-end real-time adaptive OOFDM transceivers over DML-based IMDD 25-km MetroCor SMF systems employing DACs/ADCs at sampling speeds of 4 GS/s. For PL, BL, and BPL, the measured BER against received optical power is plotted in Fig. 3(a), and in obtaining this the electrical gain at the receiver is adjusted as the received optical power setting varies to maintain the electrical signal amplitude at the ADC input at an optimum level.

Very similar BER curves for all these adaptive loading techniques are observed in Fig. 3(a). This confirms not only the effectiveness of these techniques in realizing the maximum transmission

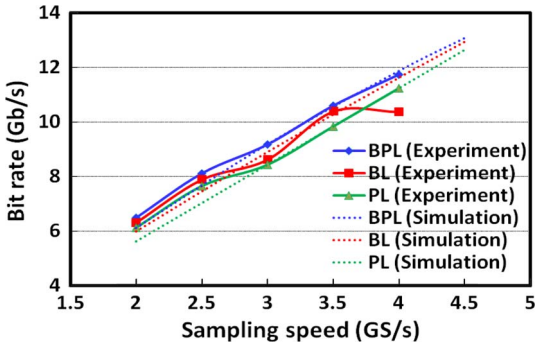

Fig. 4. Maximum signal bit rates achieved using BL, PL, and BPL as a function of DAC/ADC sampling speed over DML-based IMDD 25-km MetroCor SMF systems at received optical powers of −5.2 dBm.

performance but their capabilities in offering similar optical power budgets as well, as expected from the boundary conditions discussed in Section 4. For example, under the adopted experimental conditions listed in Section 3, for the three adaptive loading techniques, optical power budgets of $>$ 13 dB are obtainable, which are capable of accommodating roughly 16 end-users in typical OOFDM multiple access PONs. On the other hand, as mentioned in Section 1, these three adaptive loading techniques can also be utilized to further improve the aforementioned optical power budgets, if a slightly reduced signal bit rate is chosen to be the fixed parameter. This is confirmed by the differences of the residual BERs and optical power budgets between these loading techniques. As seen in Fig. 3(a), a $<$ 5% relative signal bit rate differences between different techniques can cause an optical power budget variation of approximately 3 dB.

When BPL is considered, as an example, representative constellations of single subcarriers, recorded prior to performing equalization in the receiver subject to a received optical power of −5.2 dBm, are presented in Fig. 3(b) for the first, fifth, and 15th subcarriers. These received constellations clearly show a decrease in subcarrier amplitude due to the residual system frequency response roll-off for high subcarrier frequencies, which are consistent with Fig. 2(a).

5.3. DAC/ADC Sampling Speed- and Transmission Distance-Dependent Maximum Signal Bit Rates

Over the real-time DML-based IMDD 25-km MetroCor SMF systems considered in Section 5.2, Fig. 4 shows the measured maximum signal bit rates as a function of DAC/ADC sampling speed for these three adaptive loading techniques. For comparisons with the experimental measurements, numerically simulated performances are also plotted in the same figure. In obtaining Fig. 4, for a given DAC/ADC sampling speed, independent bit and/or power loading on each individual subcarrier is performed to maximize the signal transmission capacity, corresponding to a total channel BER of 1.0×10^{-3}.

Shown in Fig. 4 and as expected from (1), the measured signal bit rates supported by different adaptive loading techniques rise almost linearly with increasing DAC/ADC sampling speed within a broad sampling speed region ranging from 2 GS/s to 3.5 GS/s. More importantly, over such a range, BPL (PL) always offers the highest (lowest) signal bit rate, and the observed absolute signal bit rate difference between BPL and PL is almost independent of DAC/ADC sampling speed. All the aforementioned experimental measurements agree very well with the numerical simulations, as seen in Fig. 4. For sampling speeds of $>$ 15 GS/s, the aforementioned absolute signal bit rate difference increases with sampling speed [11], because the adopted cyclic prefix is not sufficiently long for combating the chromatic fiber dispersion effect.

In Fig. 4, it can also be seen that, for a sampling speed of 4 GS/s, BPL supports the highest signal bit rate of 11.75 Gb/s, while BL (rather than PL) supports the lowest signal bit rate of 10.375 Gb/s. For this case only, the measured performance differs from the corresponding theoretical prediction,

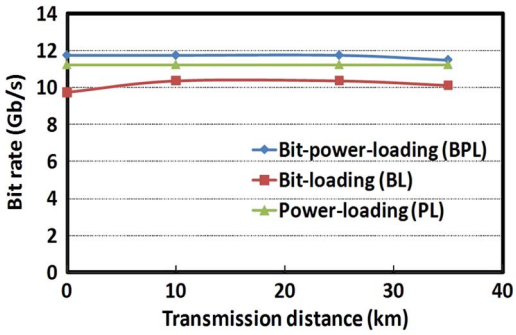

Fig. 5. Transmission distance-dependent maximum signal bit rates achieved using BL, PL, and BPL and 4 GS/s ADCs/DACs. Other system parameters are identical to those employed in Fig. 4.

TABLE 1

Consumed DSP resource comparison

	BPL	*BL*	*PL*	*Conventional***
Combinational ALUTs (72768*)	1876	1863	547	547
ALMs (36384*)	1080	1047	313	313
Dedicated logic registers (72768*)	838	835	262	262
Block memory bits (4520448*)	90920	88712	18432	17984
DSP block 9-bit elements (384*)	30	0	27	0

ALUTs: adaptive look-up tables; ALMs: adaptive logic modules;
*The number following each item in the first column indicates the available resource.
**Conventional means OOFDM using an identical signal modulation format and equal subcarrier powers

suggesting that the BL-induced lowest signal bit rate may be due to the imperfect sampling of the employed DAC/ADC at 4 GS/s, as BL is more sensitive to imperfect sampling-induced signal distortions compared with both PL and BPL.

At the fixed DAC/ADC sampling speeds of 4 GS/s, Fig. 5 shows experimentally measured signal bit rates as a function of transmission distance for various adaptive loading techniques. For all transmission distances of up to 35 km, the received optical powers are fixed at −5.2 dBm. Fig. 5 shows that BPL is capable of supporting end-to-end real-time OOFDM transmission of 11.5 Gb/s over 35-km SMFs in the systems at sampling speeds as low as 4 GS/s. By comparing Fig. 5 with Fig. 4, it is clear that all the key features shown in Fig. 4 are still retained in Fig. 5. More importantly, with the optical back-to-back case (0 km) included, the absolute signal bit rate differences between different adaptive loading techniques are almost transmission-distance independent under the conditions adopted in the experiments. This confirms that the observed signal bit rate differences originate from both the intrinsic nature of these adaptive loading techniques and fiber system-related properties.

6. Consumed Resources

According to the compilation report on consumed resources, Table 1 is given to compare resource usages for the developed real-time Altera Stratix II GX FPGA-based OOFDM transceivers incorporating BPL, BL, and PL. As a bench marker, the corresponding information for a conventional

OOFDM transceiver is also presented in the same table. Here, the conventional OOFDM transceiver is defined as the transceiver architecture using identical signal modulation formats and electrical powers on all subcarriers. To ensure fair comparison between all cases, 64-QAM is also used for both the OOFDM transceivers with PL and conventional OOFDM transceivers, and 15 information-bearing subcarriers are also considered.

It is clear from Table I that, of all these techniques considered, BPL has the highest level of resource usage across all the key elements including combinational adaptive look-up tables (ALUTs), adaptive logic modules (ALMs), dedicated logic registers, block memory bits, and DSP block 9-bit elements. While compared with BPL, the corresponding resources consumed by PL are more than three times lower, which are almost identical to those consumed by the conventional OOFDM transceivers. Such significant DSP resource usage variations arise mainly due to the difference in the number of allocated QAM modulators/demodulators for each subcarrier to choose from. For example, this number is 1 and 4 for PL and BPL, respectively. Furthermore, as both PL and BPL require a certain number of multipliers to adjust their subcarrier powers, a high usage of the DSP block 9-bit elements also occurs, but such usage is zero for both BL and the conventional technique because the multiplication operations are not required.

Given the fact that the DSP resource usage is proportional to the number of adopted information-bearing subcarriers, therefore, the concerned DSP complexity difference between various adaptive loading techniques are significantly enlarged when a large number of subcarriers are utilized in transceiver designs. In addition, great care should also be given to the maximum achievable internal clocks, which become relatively slow for high-complexity DSP designs. For example, according to the compilation report, the estimated maximum internal clocks for BPL, BL, PL, and conventional OOFDM are 134.77 MHz, 157.06 MHz, 162.10 MHz, and 176.55 MHz, respectively.

7. Conclusion

Successful experimental demonstrations have been reported of end-to-end real-time OOFDM transceivers incorporating three widely adopted adaptive loading techniques namely PL, BL, and BPL. Making use of online performance monitoring and live parameter optimization in simple DML-based IMDD transmission systems consisting of up to 35 km SMFs, extensive experimental comparisons between these three adaptive loading techniques have been made in terms of maximum achievable signal bit rate, optical power budget, and resource usage. It has been shown that BPL is capable of supporting end-to-end real-time OOFDM transmission of 11.75 Gb/s over 25-km SMFs in the aforementioned transmission systems using DAC/ADC sampling speeds as low as 4 GS/s. In addition, experimental measurements have also shown that BPL (PL) always offers the highest (lowest) signal bit rate, and their optical power budgets are similar. The absolute signal bit rate difference between BPL and PL is almost independent of DAC/ADC sampling speed and transmission distance under the experimental conditions adopted in the paper. All the aforementioned key features agree very well with numerical simulations. Moreover, BPL consumes the most DSP resources, which are approximately three times higher than those required by PL having resource usage similar to conventional OOFDM transceivers. The above results indicate that PL is a preferred option for cost-effective OOFDM transceiver architecture design.

References

[1] E. Hugues-Salas, R. P. Giddings, X. Q. Jin, J. L. Wei, X. Zheng, Y. Hong, C. Shu, and J. M. Tang, "Real-time experimental demonstration of low-cost VCSEL intensity-modulated 11.25 Gb/s optical OFDM signal transmission over 25 km PON systems," *Opt. Exp.*, vol. 19, no. 4, pp. 2979–2988, Feb. 2011.

[2] R. P. Giddings, E. Hugues-Salas, X. Q. Jin, J. L. Wei, and J. M. Tang, "Experimental demonstration of real-time optical OFDM transmission at 7.5 Gb/s over 25-km SSMF using a 1-GHz RSOA," *IEEE Photon. Technol. Lett.*, vol. 22, no. 11, pp. 745–747, Jun. 2010.

[3] J. M. Tang and K. A. Shore, "30 Gb/s signal transmission over 40-km directly modulated DFB-laser-based single-mode-fibre links without optical amplification and dispersion compensation," *J. Lightw. Technol.*, vol. 24, no. 6, pp. 2318–2327, Jun. 2006.

[4] T. Duong, N. Genay, M. Ouzzif, J. Le Masson, B. Charbonnier, P. Chanclou, and J. C. Simon, "Adaptive loading algorithm implemented in AMOOFDM for NG-PON system integrating cost-effective and low-bandwidth optical devices," *IEEE Photon. Technol. Lett.*, vol. 21, no. 12, pp. 790–792, Jun. 2009.
[5] S. K. Wilson and J. Armstrong, "Transmitter and receiver methods for improving asymmetrically-clipped optical OFDM," *IEEE Trans. Wireless Commun.*, vol. 8, no. 9, pp. 4561–4567, Sep. 2009.
[6] R. P. Giddings, X. Q. Jin, E. Hugues-Salas, E. Giacoumidis, J. L. Wei, and J. M. Tang, "Experimental demonstration of a record high 11.25 Gb/s real-time optical OFDM transceiver supporting 25 km SMF end-to-end transmission in simple IMDD systems," *Opt. Exp.*, vol. 18, no. 6, pp. 5541–5555, Mar. 2010.
[7] X. Q. Jin, R. P. Giddings, E. Hugues-Salas, and J. M. Tang, "Real-time experimental demonstration of optical OFDM symbol synchronization in directly modulated DFB laser-based 25 km SMF IMDD systems," *Opt. Exp.*, vol. 18, no. 20, pp. 21 100–21 110, Sep. 2010.
[8] H. Yang, S. C. J. Lee, E. Tangdiongga, C. Okonkwo, H. P. A. van den Boom, F. Breyer, S. Randel, and A. M. J. Koonen, "47.4 Gb/s transmission over 100 m graded-index plastic optical fiber based on rate-adaptive discrete multitone modulation," *J. Lightw. Technol.*, vol. 28, no. 4, pp. 352–359, Feb. 2010.
[9] I. B. Djordjevic and H. G. Batshon, "LDPC-coded OFDM for heterogeneous access optical networks," *IEEE Photon. J.*, vol. 2, no. 4, pp. 611–619, Aug. 2010.
[10] S. Loquai, R. Kruglov, C.-A. Bunge, O. Ziemann, B. Schmauss, and J. Vinogradov, "10.7-Gb/s discrete multitone transmission over 25-m bend-insensitive multicore polymer optical fiber," *IEEE Photon. Technol. Lett.*, vol. 22, no. 21, pp. 1604–1606, Nov. 2010.
[11] E. Giacoumidis, X. Q. Jin, A. Tsokanos, and J. M. Tang, "Statistical performance comparisons of optical OFDM adaptive loading algorithms in multimode fiber-based transmission systems," *IEEE Photon. J.*, vol. 2, no. 6, pp. 1051–1059, Dec. 2010.
[12] X. Q. Jin, R. P. Giddings, and J. M. Tang, "Experimental demonstration of adaptive bit and/or power loading for maximizing real-time end-to-end optical OFDM transmission performance," presented at the Opt. Fiber Commun. Conf., Los Angeles, CA, Mar. 2011, Paper JWA029.
[13] J. L. Wei, C. Sánchez, R. P. Giddings, E. Hugues-Salas, and J. M. Tang, "Significant improvements in optical power budgets of real-time optical OFDM PON systems," *Opt. Exp.*, vol. 18, no. 20, pp. 20 732–20 745, Sep. 2010.
[14] J. M. Tang, P. M. Lane, and K. A. Shore, "High-speed transmission of adaptively modulated optical OFDM signals over multimode fibres using directly modulated DFBs," *J. Lightw. Technol.*, vol. 24, no. 1, pp. 429–441, Jan. 2006.
[15] X. Zheng, X. Q. Jin, R. P. Giddings, J. L. Wei, E. Hugues-Salas, Y. H. Hong, and J. M. Tang, "Negative power penalties of optical OFDM signal transmissions in directly modulated DFB laser-based IMDD systems incorporating negative dispersion fibres," *IEEE Photon. J.*, vol. 2, no. 4, pp. 532–542, Aug. 2010.
[16] Z. Zan, M. Premaratne, and A. J. Lowery, "Laser RIN and linewidth requirements for direct detection optical OFDM," presented at the Conf. Lasers Electro-Optics/Quantum Electron. Laser Sci. Conf. Photonic Applications Sys. Technol., Washington, DC, 2008, Paper CWN2.
[17] G. P. Agrawal, *Fibre-Optic Communication Systems,* 2nd ed. Hoboken, NJ: Wiley, 1997.
[18] X. Q. Jin, R. P. Giddings, E. Hugues-Salas, and J. M. Tang, "Real-time demonstration of 128-QAM-encoded optical OFDM transmission with a 5.25 bit/s/Hz spectral efficiency in simple IMDD systems utilizing directly modulated DFB lasers," *Opt. Exp.*, vol. 17, no. 22, pp. 20 484–20 493, Oct. 2009.